Cloud's simulation in a 3D radiative transfer model

Author: Pol Martí Rovira, pmartiro92@alumnes.ub.edu
Facultat de Física, Universitat de Barcelona, Diagonal 645, 08028 Barcelona, Spain.

Advisor: Yolanda Sola Salvatierra, ysola@meteo.ub.edu

Abstract: Earth's energy budget is influenced by different cloud types and cloud cover. The direct interaction between clouds and radiation is usually estimated using one-dimensional (1D) radiative transfer models, whereas complex three-dimensional (3D) effects are often neglected. This study compares 1D Independent Column Approximation (ICA) simulations with 3D simulations, both based on Monte Carlo methods, and provided by the I3RC online simulator. The monochromatic reflectance at the top of the atmosphere and its dependence on the solar zenith angle provide the basis for comparing three cloud fields and different locations within a given scenario. In homogeneous cloud scenes, the 1D and 3D simulations produced nearly identical results. However, in spatially heterogeneous cloud fields, substantial differences were observed, with discrepancies reaching up to 0.3 in specific cases.
Keywords: Radiative transfer, Shortwave radiation, Monte Carlo simulations, NASA I3RC model, Inhomogeneous clouds.
SDGs: Quality education, Affordable and clean energy, Climate action.

I. INTRODUCTION

Clouds play a significant role in the Earth's energy budget. First, they reflect part of the incoming shortwave solar radiation back to space and another fraction is absorbed by cloud droplets and ice particles. Second, the Earth's surface emits longwave radiation, which is absorbed by clouds and then re-emitted both toward the surface and into space. All these processes are components of the cloud radiative effect (CRE), which is closely related to cloud feedback, an essential factor in the study of global warming [1] [2]. In addition to their role in the energy budget, clouds also modulate solar irradiance that reaches the Earth's surface and consequently other meteorological variables, such as surface temperature. Accurate estimations of solar irradiance are crucial for meteorological forecasting and applications, particularly for solar energy applications.

Aerosols also substantially influence Earth's energy budget through both direct and indirect effects. They scatter and absorb solar radiation, which can either cool the surface by reflecting energy back to space or warm the atmosphere through absorption. Furthermore, aerosols affect cloud formation by changing cloud particle size, thereby modifying cloud reflectivity and absorption of radiation. As a result, aerosols play a key role in regulating climate and atmospheric temperature.

Radiative fluxes in climate and meteorological models are typically determined using simplified versions of more complex radiative transfer (RT) models. These models are also widely used to retrieve atmospheric properties from satellite observations, such as gas or aerosol concentrations. In general, radiative fluxes are computed under the assumption of a plane-parallel atmosphere and one-dimensional (1D) RT, thus neglecting horizontal fluxes. Although these approximations are widely used, they do not consider cloud inhomogeneities and can lead to inaccuracies and large uncertainties in some conditions. More complex approaches based on three-dimensional (3D) radiative models have been developed in recent years, although the computational cost and the requirement of input parameters increase [3].

This work aims to analyze the differences in solar reflectance at the top of the atmosphere computed with 1D and 3D radiative simulations under different cloud scenarios.

II. METHODOLOGY

Most RT calculations are based on 1D deterministic models, which solve the RT equation over a set of directions. In contrast, Monte Carlo methods estimate radiative fluxes by simulating a large number of photon trajectories and then averaging the results. The Monte Carlo Independent Column Approximation (ICA) was developed to account for the variability inside the vertical column without horizontal transport.

Under cloudy conditions the horizontal transport of photons can be significant and therefore, a complete Monte Carlo approach should be considered. This motivated the creation of the Intercomparison of 3D Radiation Codes (I3RC) [4]. One of the project's goals was to compare available methods for three-dimensional atmospheric radiative transfer calculations and to provide benchmark results for testing 3D radiative transfer codes.

In the framework of the I3RC project, a web-based simplified solver was developed. Although this solver does not allow the user to perform simulations over large areas in an iterative way, it represents a useful tool to explore 3D models under cloud conditions.

A. Model description

This work has been based on the I3RC online calculator, which provides a simplified way to calculate the spatial distribution and scene-average value of radiances, fluxes, and absorption at selected visible and near-infrared wavelengths.

The I3RC online calculator enables users to configure simulations through several key parameters. Primarily, the user defines the observation geometry depending on whether the platform is satellite, airborne, or ground-based.

A fundamental feature of the I3RC tool is the choice between 3D and 1D-ICA radiative transfer settings. Moreover, users can choose the view direction, sensor location, or field of view, depending on the simulated item. The solar geometry is defined via zenith and azimuth angles, while atmospheric and surface properties, such as aerosol optical depth and surface albedo, can also be adjusted.

The computational cost can be managed by selecting simulation times ranging from 15 s to 4 min. As simulation time increases, the number of photon paths computed also grows, reducing the statistical uncertainty.

One of the output variables is the monochromatic reflectance at the top of the atmosphere (TOA), hereafter referred to simply as reflectance, defined as

$$R_\lambda = \frac{\pi I_\lambda}{\mu_0 F_{0,\lambda}} \ , \tag{1}$$

where I_λ denotes the simulated spectral radiance, expressed in $\mathrm{W\,m^{-2}\,sr^{-1}\,\mu m^{-1}}$, μ_0 represents the cosine of the solar zenith angle (SZA), and $F_{0,\lambda}$ denotes the solar spectral irradiance incident on a unit area perpendicular to the incoming solar radiation, measured in $\mathrm{W\,m^{-2}\,\mu m^{-1}}$. The reflectance assumes that radiance is equal in all directions (Lambertian approximation, πI_λ).

The simulator provides an uncertainty estimated for this output value. This uncertainty arises from the inherent statistical character of the Monte Carlo method, which relies on the simulation of random photon paths.

B. Simulation setup

This computational tool enables the simulation of a large number of cloud distributions. It operates by defining a three-dimensional grid whose dimensions can be adjusted. For each grid cell, the volume extinction coefficient (β_{e_λ}) must be specified. This parameter is a measure of the attenuation per unit distance due to absorption and scattering processes.

The optical depth (τ_λ) can be calculated as the columnar integration of β_{e_λ}:

$$\tau_\lambda = \int_{\text{column}} \beta_{e_\lambda}\, dz \ . \tag{2}$$

Under the discrete approximation used in this study, Eq. 2 can be expressed as

$$\tau_\lambda = \sum_{i=1}^{N} \beta_{e_{\lambda,i}} \Delta z \ , \tag{3}$$

where N denotes the number of cells in the column, i is the index iterating over the cells, and Δz represents the vertical cell thickness. The optical depth includes the extinction by clouds but also by gases and aerosols in the column. Furthermore, cloud base height (CBH) grid is adjustable, providing users with flexibility to model various realistic cloud fields.

The main I3RC interface provides a cloud library, from which three configurations have been selected for this study. All three scenarios were analyzed using 15 s simulations at a wavelength of 0.65 µm, corresponding to red light, which is commonly employed in cloud observations. The simulations were performed for a nadir-viewing sensor and the sun positioned to the south. Moreover, under the Lambertian assumption, an underlying surface albedo of 5% was selected, which represents vegetation-covered surfaces.

The first cloud field employed in our research consists of a homogeneous low-level cloud represented by a single cubic cell with a side length of 1000 m and a CBH of 500 m. The optical depth for this cell is $\tau = 5$. The second cloud field corresponds to I3RC case 4 from the cloud library and represents a cloud field formed by cumulus clouds. The scenario is represented on a 3D grid of $100 \times 100 \times 36$ cells, with individual cell dimensions of $67 \times 67 \times 40$ m in the x-, y- , and z-direction, respectively, resulting in a total grid size of $6700 \times 6700 \times 1440$ m, with a CBH of 1000 m. Figure 1a shows the spatial distribution of the optical depth on the grid. The third cloud field corresponds to I3RC case 5 from the cloud library and represents a field of stratocumulus clouds. It is constructed from a grid of $64 \times 64 \times 16$ cells, each measuring $55 \times 55 \times 25$ m, yielding overall grid dimensions of $3520 \times 3520 \times 400$ m, with a CBH of 400 m. Figure 1b shows the spatial distribution of the optical depth on the grid.

Points 2.1 and 3.1, from Figures 1a and 1b, respectively, are predefined reference locations in the I3RC cloud scenarios analyzed, whereas the remaining points were selected to characterize the cloud field and highlight its inhomogeneity. In the next section, these points will be used as a reference for the discussion.

Tables Ia and Ib list the exact coordinates of every point in the xy-plane together with the corresponding vertical optical depth values.

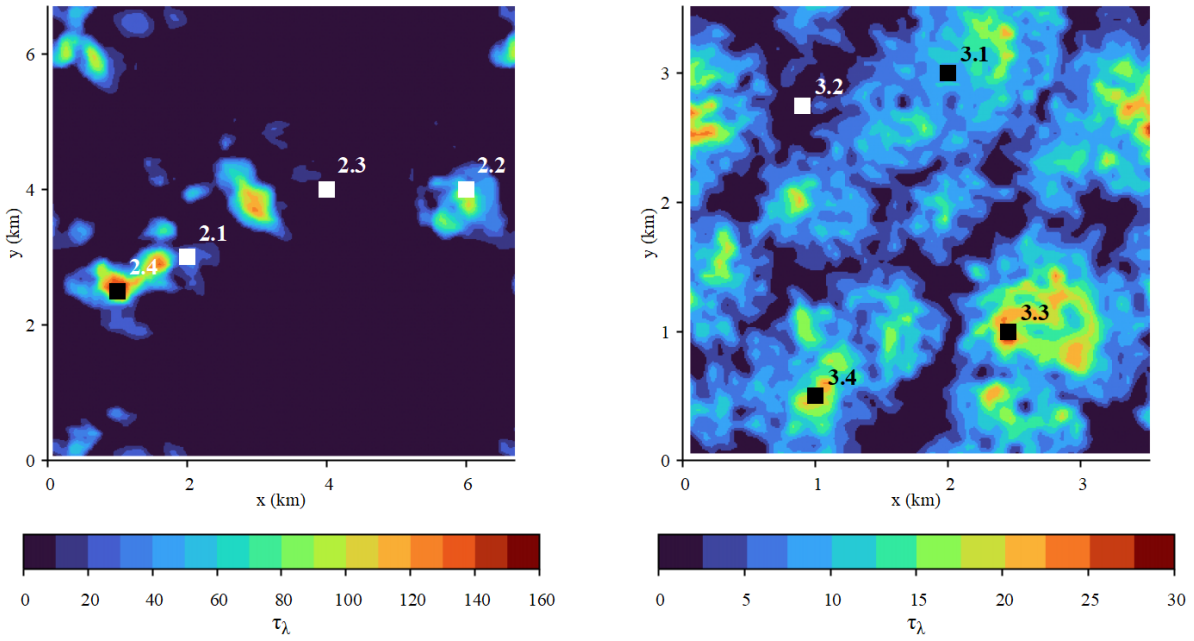

(a) Cloud field 2.

(b) Cloud field 3.

FIG. 1: Spatial distribution of column optical depth at $\lambda = 0.65$ µm in the cloud field xy-plane. The scale is properly adapted in each figure. The optical depth values for the four points marked in each figure are shown in Tables Ia and Ib.

TABLE I: Optical depth values at $\lambda = 0.65$ µm for every point marked in Figures 1a and 1b.

(a) Cloud field 2.

Label	(x,y) (km)	τ_λ
2.1	(2,3)	30.72
2.2	(6,4)	94.96
2.3	(4,4)	1.10
2.4	(1,2.5)	136.54

(b) Cloud field 3.

Label	(x,y) (km)	τ_λ
3.1	(2,3)	8.65
3.2	(0.9,2.75)	0.61
3.3	(2.45,1)	26.35
3.4	(1,0.5)	19.08

III. RESULTS AND DISCUSSION

The clouds studied in the three scenarios exhibit markedly different characteristics. The homogeneous cloud represents an idealized case and serves as the basis for comparison. The second scenario is characterized by cumulus clouds with high optical depths and notable vertical development. As a result, the cloud field is highly inhomogeneous. In contrast, the third scenario consists of a stratocumulus cloud field with lower optical depths and reduced vertical development, resulting in a more homogeneous cloud structure.

Figure 2 shows the dependence of reflectance at TOA on SZA over (x, y) = (2, 3) km (points labeled 2.1 and 3.1 in Figures 1a and 1b, respectively) for 1D and 3D approaches in the three cases. Reflectance decreases monotonically with increasing SZA, owing to the increasing angular separation between the viewing direction and the solar direction. This behavior is related to the photon path length. According to Beer's law, the monochromatic intensity, and therefore the reflectance, decreases monotonically with increasing path length as the radiation propagates through the layer and experiences multiple scattering events.

Regarding differences between 1D and 3D results, for the homogeneous cloud, the values are nearly identical with negligible differences associated with Monte Carlo sampling noise resulting from the number of photons used in each simulation. In contrast, the cumulus and stratocumulus cloud fields show greater differences in reflectance. In cloud field 2, point 2.1 (Figure 1a) is located in a highly inhomogeneous region of the cloud field, resulting in a noticeably larger 1D–3D discrepancy. Comparing the three scenarios in Figure 2, the results show that larger reflectances are associated with higher optical depths (Table I). Additionally, this result can be attributed to the relative inhomogeneity surrounding points 2.1 and 3.1 (Figures 1a and 1b). Uncertainties are almost negligible for the homogeneous cloud, whereas they become larger in the cumulus and stratocumulus cases. This increase is associated with higher reflectance values and enhanced 1D–3D differences.

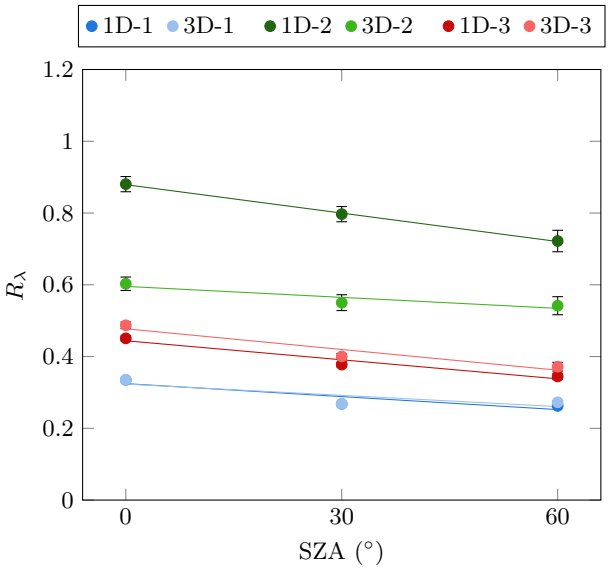

FIG. 2: Reflectance at $\lambda = 0.65$ µm for different solar zenith angles for the three scenarios described. The notation "1D-1" denotes the reflectance calculated using a one-dimensional simulation for cloud field 1. The y-error bars represent the uncertainty associated with the simulation, as provided by the model. The regression lines are shown only as visual guides to the trends in the data.

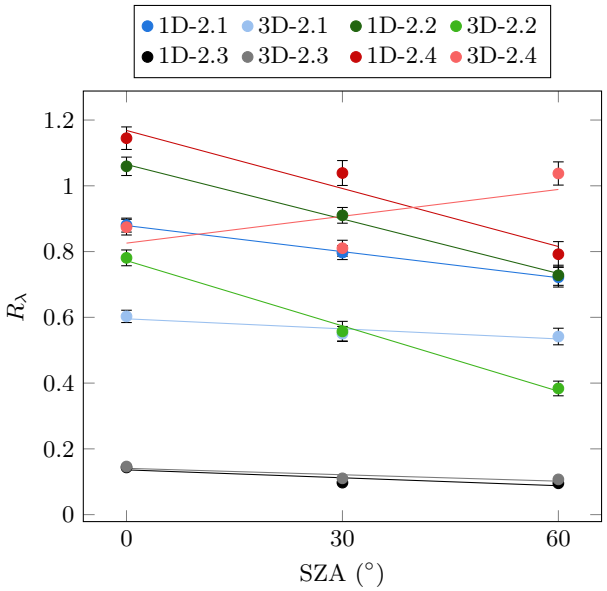

FIG. 3: Reflectance at $\lambda = 0.65$ µm for different solar zenith angles for the four points analyzed in Figure 1a. The notation "1D-2.1" denotes the reflectance calculated using a one-dimensional simulation for point labeled as 2.1. The y-error bars represent the uncertainty associated with the simulation, as provided by the model. The regression lines are shown only as visual guides to the trends in the data.

Figures 3 and 4 show the reflectances at different locations in scenarios 2 and 3, respectively. Regarding Figure 3, points such as 2.3, which lie within a homogeneous region of the cloud field 2 (Figure 1a), show almost identical 1D and 3D reflectance values. As mentioned previously, this very small discrepancy, which is shown in Table II, is caused by the number of photons used in the simulation. Other points located in more inhomogeneous regions (2.1 and 2.2) exhibit a decreasing trend with increasing SZA, along with substantial differences between the 1D and 3D reflectance values, as shown by the discrepancies in Table II. Additionally, larger values are linked to higher optical depths. Point 2.4, located in a highly inhomogeneous region with a large optical depth, shows an increase in reflectance with increasing SZA in the 3D approach, whereas the 1D reflectance exhibits an opposite trend, as indicated by the 1D–3D ratio in Table II. This result suggests a strong influence of the surrounding columns in this case. For 1D simulations, as the SZA increases the path length is longer enhancing extinction processes in the column. In contrast, for 3D simulations the horizontal photon transport from adjacent optically thick columns can compensate the longer path length.

The reflectances at points 2.2 and 2.4 exceed 1, which is consistent with the definition of reflectance. This quantity is defined assuming an ideal Lambertian reflector, whereas the radiation emerging from optically thick cloud is anisotropic due to multiple scattering and weak absorption.

TABLE II: Ratio between 1D and 3D reflectances (1D/3D) and their discrepancy for different solar zenith angles (SZA). Data are shown for every point in Figure 1a (cumulus scenario). Discrepancy is calculated by subtracting 3D from 1D reflectance.

Label	Location (km)	SZA (°)	1D/3D	Discrepancy
2.1	(2,3)	0	1.460	0.287
		30	1.448	0.247
		60	1.333	0.180
2.2	(6,4)	0	1.357	0.278
		30	1.634	0.353
		60	1.897	0.344
2.3	(4,4)	0	0.981	-0.003
		30	0.881	-0.013
		60	0.889	-0.012
2.4	(1,2.5)	0	1.310	0.271
		30	1.282	0.229
		60	0.763	-0.246

For cloud field 3 (Figure 4), point 3.2 presents only minor differences between the 1D and 3D reflectance values. As observed in cloud field 2, points with low optical depth (Table 1b) located in homogeneous regions (Figure 1b) tend to show nearly identical reflectance in the 1D and 3D approaches.

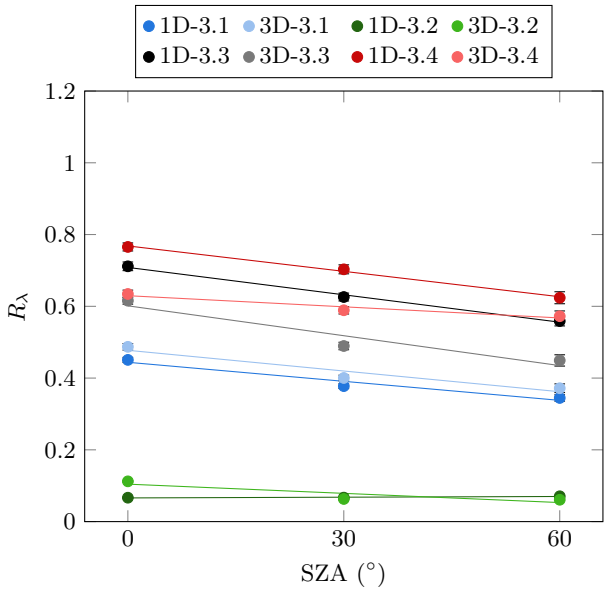

FIG. 4: As Figure 3, but for the four points analyzed in Figure 1b.

TABLE III: As Table II, but for every point in Figure 1b (stratocumulus cloud field).

Label	Location (km)	SZA (°)	1D/3D	Discrepancy
3.1	(2,3)	0	0.925	-0.036
		30	0.943	-0.023
		60	0.927	-0.027
3.2	(0.9,2.75)	0	0.594	-0.046
		30	1.059	0.004
		60	1.159	0.010
3.3	(2.45,1)	0	1.156	0.096
		30	1.279	0.137
		60	1.244	0.110
3.4	(1,0.5)	0	1.207	0.131
		30	1.194	0.114
		60	1.090	0.052

Points 3.3 and 3.4 exhibit the same decreasing trend, as quantified by the 1D–3D ratio reported in Table III. As highlighted in the second scenario, points situated in sufficiently inhomogeneous regions show larger discrepancies between the 1D and 3D reflectance values, with the 1D reflectance exceeding the 3D reflectance. This result suggests that the 1D approach overestimates the reflectance. Point 3.1 exhibits a similar behavior, although the 3D reflectance is greater than the 1D reflectance. However, the difference between the two values is relatively small, as shown by the discrepancy in Table III.

Taken together, the results reported in Figures 3 and 4 indicate that, when reflectance is computed over inhomogeneous regions, 1D simulations either overestimate the reflectance or produce values that differ markedly from those obtained with 3D simulations.

IV. CONCLUSIONS

The analysis of the reflectance at the top of the atmosphere simulated with 3D and 1D-ICA Monte Carlo models has allowed us to conclude: 1D simulations have limitations in accurately representing reflectance in cloudy scenes, highlighting the importance of 3D approaches.

Substantial discrepancies between 1D and 3D reflectance are observed, particularly in highly inhomogeneous cloud regions. In stratocumulus cloud fields, these discrepancies are even larger than those found in homogeneous and cumulus cloud fields. In some cases, the discrepancy between the 1D and 3D reflectance reaches nearly 0.3, while the corresponding 1D and 3D trends exhibit opposite behaviors.

Nonetheless, this study is only a first step toward demonstrating the benefits of considering three-dimensional cloud structures. A natural improvement would be to analyze the complete reflectance field rather than focusing on isolated points.

Acknowledgments

I would like to thank my supervisor, Yolanda Sola, for her valuable guidance and insightful advice. I would also like to thank Dr.Várnai for providing access to the I3RC online simulator. Finally, I would like to thank my family, colleagues, and friends for their ongoing support throughout this work.

[1] Ceppi, P., and P. Nowack, 2021: Observational evidence that cloud feedback amplifies global warming. *Proc. Natl. Acad. Sci. U.S.A.*, **118**, e2026290118, https://doi.org/10.1073/pnas.2026290118.

[2] IPCC, 2021: *Climate Change 2021: The Physical Science Basis. Contribution of Working Group I to the Sixth Assessment Report of the Intergovernmental Panel on Climate Change*. V. Masson-Delmotte et al., Eds., Cambridge University Press, https://doi.org/10.1017/9781009157896.

[3] Barker, H. W., S. Kato, and T. Wehr, 2012: Computation of solar radiative fluxes by 1D and 3D methods using cloudy atmospheres inferred from A-train satellite data. *Surv. Geophys.*, **33**, 657-676, https://doi.org/10.1007/s10712-011-9164-9.

[4] Cahalan, R.F., and Coauthors. 2005: The I3RC: Bringing together the most advanced radiative transfer tools for cloudy atmospheres. *Bull. Amer. Meteor. Soc.*, **86**, 1275-1293, https://doi.org/10.1175/BAMS-86-9-1275.

Simulació de núvols en un model 3D de transferència radiativa

Author: Pol Martí Rovira, pmartiro92@alumnes.ub.edu
Facultat de Física, Universitat de Barcelona, Diagonal 645, 08028 Barcelona, Spain.

Advisor: Yolanda Sola Salvatierra, ysola@meteo.ub.edu

Resum: El balanç radiatiu de la Terra es veu influenciat per diferents tipus de núvols i per la seva cobertura. La interacció directa entre núvols i radiació se sol estimar mitjançant models unidimensionals (1D) de transferència radiativa, mentre que sovint es menyspreen els complexos efectes tridimensionals (3D). Aquest estudi compara simulacions 1D basades en l'Aproximació de Columna Independent (ICA) amb simulacions 3D, ambdues basades en mètodes de Monte Carlo i proporcionades pel simulador en línia I3RC. La reflectància monocromàtica al cim de l'atmosfera i la seva dependència de l'angle zenital solar constitueixen la base de la comparació entre tres camps de núvols i entre diferents ubicacions dins d'un mateix escenari. Per núvols homogenis, les simulacions 1D i 3D van dur a resultats gairebé idèntics. Tanmateix, en camps de núvols espacialment heterogenis es van observar diferències rellevants, amb discrepàncies de fins a 0.3 en casos concrets.
Paraules clau: Transferència radiativa, Radiació d'ona curta, Simulacions Monte Carlo, Model NASA I3RC, Núvols inhomogenis.
ODSs: Educació de qualitat, Energia neta i sostenible, Acció climàtica.

Objectius de Desenvolupament Sostenible (ODSs o SDGs)

1. Fi de les desigualtats		10. Reducció de les desigualtats	
2. Fam zero		11. Ciutats i comunitats sostenibles	
3. Salut i benestar		12. Consum i producció responsables	
4. Educació de qualitat	X	13. Acció climàtica	X
5. Igualtat de gènere		14. Vida submarina	
6. Aigua neta i sanejament		15. Vida terrestre	
7. Energia neta i sostenible	X	16. Pau, justícia i institucions sòlides	
8. Treball digne i creixement econòmic		17. Aliança pels objectius	
9. Indústria, innovació, infraestructures			

Aquest TFG s'inscriu en l'ODS 4, ja que contribueix a la divulgació de contingut tècnic a estudiants. També, es pot relacionar amb l'ODS 7, perquè l'estudi de la influència dels núvols i de la seva cobertura en el balanç radiatiu terrestre ens permet estimar millor la irradiància solar, el coneixement de la qual és de gran utilitat per l'aprofitament de l'energia solar. En relació amb l'ODS 13, un dels factors que propicia l'escalfament global són els canvis en el balanç radiatiu dels núvols i aquest estudi pretén millorar-ne la determinació.